

1 **Different migration patterns of European anchovy and sardine around Iberian
2 Peninsula revealed by eye lens isotopes**

3 **Authors**

4 Tatsuya Sakamoto^{1,2*} and Susana Garrido¹

5 **Affiliations**

6 1. Instituto Português do Mar e da Atmosfera, Lisbon, Portugal

7 2. The Hakubi Center for Advanced Research, Kyoto, Japan

8 *Corresponding author

9 Email: sakamoto.tatsuya.3p@kyoto-u.ac.jp

10 Present address: Yoshidanihonmatsucho, Kyoto Sakyo-ku, Kyoto, 606-8316 Japan

11 **Keywords**

12 Eye lens, stable isotope, migration, population structure, anchovy, sardine, fishery
13 management

14 **Highlights**

15

- The first movement analysis using eye lens isotopes for European anchovy and
16 sardine
- Anchovy populations were separated between west and south Iberian coasts
- In contrast, sardine was mixed considerably between west and south coasts
- Trans-boundary connectivity between west and north coasts may exist in anchovy
- Inferences from eye lens isotopes will help fisheries management under climate
17 change

18 **Abstract**

19 Small pelagic fish are key components of productive coastal ecosystems, yet their
20 migration ecology remains poorly understood, causing challenges for management. We
21 applied stable carbon and nitrogen isotope ($\delta^{13}\text{C}$ and $\delta^{15}\text{N}$) analyses of eye lenses to
22 investigate movements of European anchovy (*Engraulis encrasicolus*) and sardine
23 (*Sardina pilchardus*) around the Iberian Peninsula. Muscle isotopes showed strong spatial
24 heterogeneity, largely consistent between species and reflecting differences in baseline
25 values. Eye lens centres of small anchovy, and to a lesser extent sardine, also showed
26 clear geographic variation: higher $\delta^{15}\text{N}$ off the Atlantic south coast, lowest $\delta^{15}\text{N}$ in the

37 Alboran Sea, and lower $\delta^{13}\text{C}$ off the west coast. These patterns persisted across years and
38 fish sizes in anchovy, with only minor outliers, suggesting limited cross regional
39 migration. An exception was the overlap between west coast and Cantabrian Sea values,
40 consistent with connectivity supported by cohort tracking. In contrast, sardine isotopes
41 from the west and south coasts converged into a unimodal distribution with growth,
42 indicating frequent exchange between these regions. These findings support recent
43 revision of stock limits that separate south and west coast anchovy stocks and maintain a
44 single Iberian sardine stock, but they question the current assumption of separation
45 between western and northern anchovy stocks. Eye lens isotopes provide a powerful
46 complementary tool to resolve nursery origin and connectivity, offering new opportunities
47 for fisheries management in shorter time scales than molecular techniques, which is
48 paramount to be able to cope with rapid changes of fish distribution due to climate change,
49 and for spatially explicit management.

50

51 **Introduction**

52 Marine fish often change their habitats with ontogeny and seasons to avoid predation,
53 meet physiological requirements and maximise fitness, resulting in diverse migration
54 patterns among and within species or populations (Bauer and Hoye, 2014). Resolving
55 each unique migration pattern is critical for defining management boundaries and
56 assessing connectivity (Frisk et al., 2013), which is key for developing effective
57 management practices. Stock assessment models, that provide the framework for setting
58 exploitation limits, often rely on the assumption of well-mixed, self-recruiting population
59 within boundaries (Cadrin et al., 2023). Connectivity determines whether local
60 populations persist through self-recruitment or depend on external sources, with direct
61 consequences for resilience to environmental change and fishing pressure (Sakamoto et
62 al., 2024). Misspecifications of boundaries or inaccurate estimation of connectivity can
63 therefore lead to biased assessments (Berger et al., 2021), overexploitation and stock
64 collapses (Petitgas et al., 2010). Mass migrations of fish can also have substantial
65 ecological impacts on ecosystems through alterations of energy flow, food-web topology
66 and stability, and trophic cascades (Bauer and Hoye, 2014). Understanding migration
67 patterns of abundant species and its ecological function should significantly contribute to
68 ecosystem-based managements (Link et al., 2020).

69

70 European anchovy *Engraulis encrasicolus* and European sardine *Sardina pilchardus* are
71 key components in the Northeast Atlantic and Mediterranean shelf ecosystems. These
72 small pelagic fishes are short-lived and abundant plankton feeders (Garrido et al., 2015)

73 and, being fed by many predators including fish (Cardona et al., 2015), mammals (Santos
74 et al., 2014) and seabirds (Martínez-Abraín et al., 2019), they play a critical role in energy
75 transfer from low to high trophic levels (Veiga-Malta et al., 2019). They are also important
76 targets of pelagic fisheries, particularly off Western Moroccan waters and around the Bay
77 of Biscay and Iberian Peninsula, providing several hundred thousand tonnes of landing
78 annually (FAO 2025). However, the sustainability of the fishery is challenged by
79 biological changes in recent years, such as a reduction of body sizes of both species in
80 the Bay of Biscay (Véron et al., 2020; Taboada et al., 2024), declined sardine abundance
81 off the Iberian west coast where anchovy bloomed for the first time since it started being
82 recorded (Ferreira et al., 2023; 2024). Their migrations can cause significant changes in
83 trophic structures, predator distribution and abundance, and increase challenges for
84 fishery management. Despite their importance, the migration ecology of both species
85 remains poorly studied, primarily due to the lack of appropriate techniques to track
86 individual movements.

87

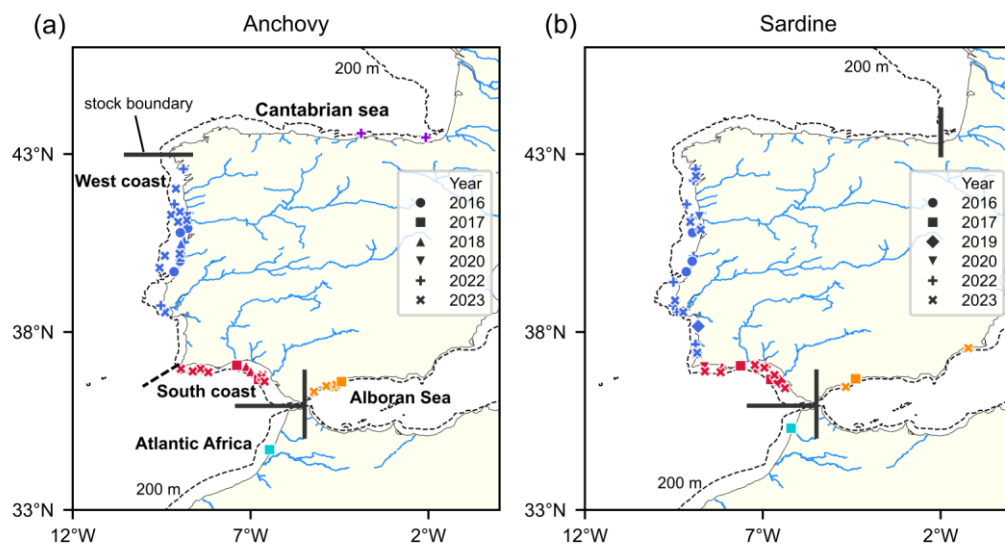
88 Population structure of the two species have been studied mainly by using genomics and
89 morphological traits (e.g., Zarraonaindia et al., 2012), although many issues remain
90 regarding the connectivity of Iberian Peninsula populations (Caballero-Huertas et al.,
91 2022a). Currently, different anchovy stocks are assumed in the Bay of Biscay, western
92 Iberian coast (hereafter West coast), and south Iberian coast (hereafter, the South coast),
93 Alboran Sea and Atlantic Africa (three different stocks assessed by FAO) for management
94 (Fig. 1). The border between the anchovy populations inhabiting the West and South
95 coasts has been added only recently (ICES, 2024a), which was supported by a compilation
96 of published and unpublished evidences from genomics, larval dispersal, fish and
97 fisheries distribution, morphometric and genomic studies (Garrido et al., 2024) but would
98 benefit from further analysis. In particular, potential connectivity between the populations
99 of the West coast and the Bay of Biscay has been suggested recently (Teles-Machado et
100 al., 2024; Pujolar et al., 2025), against the current assumption of two different stocks in
101 these areas. Adding another layer of complexity, two genetically and morphologically
102 distinct ecotypes, namely marine and coastal ecotypes, have been identified in anchovies
103 in the Mediterranean, Bay of Biscay and the North Sea (Le Moan et al., 2016; Huret et
104 al., 2020). The former thrives preferentially in pelagic systems and the latter in estuaries
105 and lagoons, whose distributions and proportions in other regions are unknown.

106

107 Sardine in the Cantabrian Sea, West and South coasts is managed as one stock (Fig. 1).
108 This is consistent with the genomic analyses that assigned those surrounding the Iberian

109 Peninsula into a single cluster (da Fonseca et al., 2024; Sabatino et al., 2025), and cohort
110 tracking analysis that suggests that the connectivity across these regions is mediated by
111 migrating adults (Silva et al., 2019). Meanwhile, morphometric analysis suggests the
112 existence of several clusters between the northern and southern Iberia (Neves et al., 2023),
113 and the connectivity between west and east of the Strait of Gibraltar have been indicated,
114 with unknown extent (Caballero-Huertas et al., 2022b; Hidalgo et al., 2024).

115



116

Figure 1. Sampling locations of anchovy (a) and sardine (b) used for isotope analyses, with representation of stock boundaries (black lines), 200 m bathymetric contour and major rivers. The broken line shows the new stock boundary added recently between west and south coast populations (a). River positions were taken from Global River Width from Landsat dataset (Allen and Pavelsky, 2018).

117

118

119

120 Stable isotopes in eye lenses may provide a complementary measure of fish movements,
121 which can be a particularly helpful tool to understand the migrations of abundant small
122 pelagic fish. Eye lenses are incrementally growing protein structure that lack turnover
123 (Wallace et al., 2014), and therefore the history of isotopes of diet are recorded in their
124 layers i.e. laminae with some isotopic offsets (Yoshikawa et al., 2025). The carbon and
125 nitrogen stable isotopes of marine organisms often show significant gradients across
126 oceanographic conditions and from inshore to offshore (Minagawa and Wada 1986; Rau
127 et al., 1989; Montoya and McCarthy, 1995), reflecting differing primary producer

128 isotopes and dietary plasticity (Bode et al., 2007; Chouvelon et al., 2015; Sakamoto et al.,
129 2023b). Thus, the isotopes recorded in eye lenses can be used as a marker of organisms'
130 locations (Vecchio and Peebles, 2022; Sakamoto et al., 2023a; 2025), making them one
131 of the rare natural tags applicable to full-marine systems where water chemistry is largely
132 homogenous. Sequential analysis from the inner to outer laminae to infer ontogenetic
133 habitat and trophic changes has been the major usage, although analysing only the central
134 part as a marker of nursery origin can be beneficial to analysis broad scale mixing from
135 larger datasets (Vecchio and Peebles, 2022; Sakamoto et al., 2025). As eye lenses can be
136 delaminated manually, the analysis is less time-consuming and equipment-dependent
137 when compared to conventional otolith chemical analyses that requires substantial sample
138 preparation efforts. This analysis can also detect movements on an ecological timescale
139 that is directly relevant to management, which distinguishes it from genetic markers that
140 indicate connectivity on an evolutionary timescale. However, overlapping isotope values
141 do not necessarily lead to the same nursery, as organisms from distinct locations can show
142 similar isotope values from different dynamics. This limitation should be considered,
143 being preferable to complement this method with other approaches, to accurately
144 understand mixing processes.

145

146 In this study, we investigated migration patterns of European anchovy and sardine around
147 the Iberian Peninsula. To understand the geographical variations of $\delta^{13}\text{C}$ and $\delta^{15}\text{N}$ of their
148 diets, muscles isotopes were first analysed. The isotopes of eye lens centre, which reflect
149 the diet isotopes during early life stages, were then analysed for the two species across
150 different size classes, to infer their nursery origin and detect ontogenetic migrations
151 between areas. To aid the inferences obtained from eye lens analysis, we also investigated
152 the connectivity by cohort tracking, comparing the abundance at ages of anchovy from
153 the Cantabrian Sea, West coast and South coast, estimated during acoustic surveys in the
154 last 10 years and interpreting the results in light of previously published results of sardine
155 cohort tracking (Silva et al. 2019).

156

157 The water surrounding the Iberian Peninsula includes regions of distinct oceanographic
158 conditions. The West coast of the Peninsula is a highly productive region, as a
159 consequence of strong and frequent upwelling events, particularly during spring and
160 summer, and due to freshwater discharge by several rivers and rías, particularly during
161 fall and winter months (Ferreira et al. 2021). The Cantabrian Sea, in the north, is the
162 transition zone between the western upwelling region and strong freshwater input in the
163 eastern end, and has lower and more variable productivity compared to western waters.

164 The southern Atlantic coast including the Gulf of Cadiz, hereafter the South coast, is
165 generally warm and oligotrophic except for some local upwelling and freshwater-input
166 spots (Lafuente and Ruiz, 2007). The Alboran Sea in the east of the Strait of Gibraltar is
167 even warmer in summer to which a jet current persistently flows (Hidalgo et al., 2024).
168 Located further south is the northwest African coast, whose Atlantic side is a coastal area
169 with permanent upwelling, and is more productive and warmer than the Iberian west coast.
170 This environmental heterogeneity offers a unique opportunity to study how European
171 anchovy and sardine move across different oceanographic conditions.

173 **Material and Methods**

174 *Sample collection*

175 European anchovy and sardine samples for stable isotope analysis were collected during
176 acoustic and trawl surveys during 2016 to 2023 conducted by multiple institutes, which
177 includes the spring acoustic survey PELAGO off Atlantic west and south Iberian coasts
178 (2016, 2018, 2020, 2022, 2023), the autumn acoustic recruitment survey IBERAS off the
179 west coast (2018, 2022, 2023), the autumn demersal survey IBTS off the west coast,
180 summer MEDIAS survey in the Alboran Sea (2023), SARLINK 1117 winter survey
181 covering the Alboran Sea, Atlantic African coast and south Iberian coast (2017), and
182 PELACUS spring survey in the Cantabrian Sea (2022). A total of 691 anchovy and 590
183 sardine specimens were available. After measuring the total length (TL), wet weight and
184 gonad weight and recording sex, white muscle tissues were extracted from dorsal side
185 and stored in 1.5 ml plastic tubes. Eye lenses were also extracted from both eyes and
186 stored in 96-well plates. Muscle and eye lenses were frozen at -20°C until later use. Fish
187 were then classified into three size ranges, small (< 120 mm TL for anchovy and < 140
188 mm TL for sardine), medium (120–140 mm and 140–180 mm, respectively) and large
189 (>140 mm and >180 mm, respectively), which roughly correspond to typical sizes of age
190 0, 1 and ≥ 2 of each species around Iberian Peninsula with 1–2 errors (Uriarte et al., 2016;
191 Silva et al., 2008).

193 *Analysis of muscles*

194 To understand the geographical variations of stable isotopes of the diet, the $\delta^{15}\text{N}$ and $\delta^{13}\text{C}$
195 of muscles were analysed for a subset of the samples. As fish of similar sizes in the same
196 haul often have similar values (Sakamoto et al., 2023b), up to six individuals per size
197 range were selected. In total, 106 anchovy from 18 hauls and 112 sardine from 19 hauls
198 collected in 2016, 2017, 2022 and 2023 were selected for the isotope analysis to cover
199 the geographical and temporal range of the target. Muscle tissues were freeze-dried and

200 ground into powder. Lipids were extracted using a 2:1 chloroform:methanol solution,
201 freeze-dried again and 800 µg of a subsample was extracted. The $\delta^{15}\text{N}$ and $\delta^{13}\text{C}$ values of
202 the samples were analysed at GeoScience Laboratory (Nagoya, Japan) using a
203 continuous-flow stable isotope ratio mass spectrometer (IsoPrime100, Elementar,
204 Stockton, UK) coupled to an elemental analyser (vario MICRO cube, Elementar;
205 FLASH2000, Thermo Fisher Scientific, Yokohama Japan). The $\delta^{15}\text{N}$ and $\delta^{13}\text{C}$ values
206 were reported in δ -notation against the atmospheric N_2 standard and the VPDB reference
207 standard (Vienna Pee Dee Belemnite), respectively, and given as a ‰ value. Analytical
208 precisions assessed by repeated measurements of laboratory standards were $\pm 0.2\text{‰}$ for
209 $\delta^{15}\text{N}$ and $\delta^{13}\text{C}$.

210

211 *Analysis of eye lenses*

212 Thawed eye lenses were placed on a slide glass under a stereo microscope with a
213 micrometre scale for delamination. Using forceps, gelatinous cortex was removed and
214 outer laminae were peeled off until the diameter of the remaining lens became smaller
215 than 1 mm, typically 0.7 to 0.9 mm, under 10–20X magnification. The eye lens centre
216 diameter corresponds to a fish size of 3 to 4 cm SL, for Japanese sardine (Sakamoto et al.,
217 2025), which has similar morphology with European sardine and anchovy. The remaining
218 centre part was rinsed with distilled water to remove potentially tangled fibres from outer
219 laminae, then attached to the inner wall of 1.5 ml tube. After drying the lens centres for
220 more than a day at a room temperature, tube lids were sealed, then the samples were sent
221 to Stable Isotopes Analysis Facility, Sciences Faculty at the University of Lisboa, Portugal.
222 Samples were weighted, then $\delta^{15}\text{N}$ and $\delta^{13}\text{C}$ were determined by continuous flow isotope
223 mass spectrometry, on a Sercon Hydra 20-22 (Sercon, UK) stable isotope ratio mass
224 spectrometer, coupled to a EuroEA (EuroVector, Italy) elemental analyser for online
225 sample preparation by Dumas-combustion. The $\delta^{15}\text{N}$ and $\delta^{13}\text{C}$ values were reported in δ -
226 notation against the atmospheric N_2 standard and the VPDB reference standard (Vienna
227 Pee Dee Belemnite), respectively, and given as a ‰ value. Analytical precisions
228 calculated using repeated measurements of laboratory standard in every batch of analysis
229 were $\leq 0.2\text{‰}$ for $\delta^{15}\text{N}$ and $\delta^{13}\text{C}$.

230

231 *Correction of eye lens isotope values*

232 As larger fish tend to have higher $\delta^{13}\text{C}$ and $\delta^{15}\text{N}$ values due to the increase of trophic
233 position, higher eye lens isotopes are expected in larger eye lens centres. To account for
234 size variations in the peeled eye lens centre, effects of sample dry weight on isotope values
235 were assessed using linear models including fish sampling region as a factor for each

236 species ($\delta^{13}\text{C}$ or $\delta^{15}\text{N} \sim \text{Region} + \text{Sample weight}$). When a significant effect of sample
237 weight was detected, which was the case for $\delta^{13}\text{C}$ and $\delta^{15}\text{N}$, the isotope values were
238 corrected to the value at 0.3 mg of sample weight using the estimated slope.

239

240 *Data analysis*

241 Consistent analysis flow was used for the two species to reveal their different migration
242 ecologies. To confirm that the isotopes values of eye lens centre are linked to nursery area,
243 the geographical differences in the value distributions were visualised using scatter plots
244 and kernel density estimations for each fish size class (small, medium, large). If many
245 fishes migrated to different regions with growth, this would result in significant changes
246 of data distributions between size classes. The temporal stability as a marker of nursery
247 origin was assessed by calculating the mean isotope values of small-sized anchovy and
248 sardine for each sampling year. Geographical variations of eye lens isotopes of
249 small–medium-sized fish were compared to those of muscles of small–medium sized fish
250 to test whether the eye lens isotopes reflect prey isotopes in each region. The inclusion of
251 medium sized fish here was to cover regions with limited number of small fishes available.

252

253

254 To investigate the temporal variations in the extent of fish mixing/separation, overlaps of
255 eye lens isotope value distributions were quantified between each group of sampling
256 region/sampling year/fish size. For each pair of groups, two-dimensional histogram with
257 0.5 and 1.0‰ bins for $\delta^{13}\text{C}$ and $\delta^{15}\text{N}$ respectively, reflecting the greater variations in $\delta^{15}\text{N}$,
258 were calculated for each group. For each bin, the smaller proportion between the two
259 groups was retained, and the sum of these across all bins provided a metric of
260 distributional overlap. While this allows the visualisation of major mixing/separations in
261 a group level, minor differences between individuals of different origins can be of
262 significant importance in terms of gene flow cannot be detected. As a complement, data
263 points outside the 95% or 99% confident ellipses, calculated based on Mahalanobis
264 distance, for fish across all size classes in each region were considered outliers. When
265 outliers were just one in a given station, they were considered potential analytical errors
266 and discarded. When multiple outliers were detected for a given station, they were
267 considered valid and used for further analysis. The nursery origins of the valid outliers
268 were inferred based on main data distributions of other sampling regions, defined as the
269 50% probability mass area of kernel density estimation, and their muscle isotope values
270 when available.

271

272 *Cohort tracking analysis*

273 To contrast our results with observations of potential source and sink areas based on
274 cohort analysis, we used published literature for the sardine (Silva et al. 2019) and
275 conducted a cohort tracking analysis for the anchovy. Particularly, we compared the
276 abundance at age of anchovy between contiguous areas using estimates of two
277 complementary spring acoustic surveys used for stock assessment: PELACUS, conducted
278 in the Cantabrian Sea and Western Galician waters and PELAGO, conducted in the
279 Western Portuguese coast and South Iberia, including the Spanish Gulf of Cadiz.

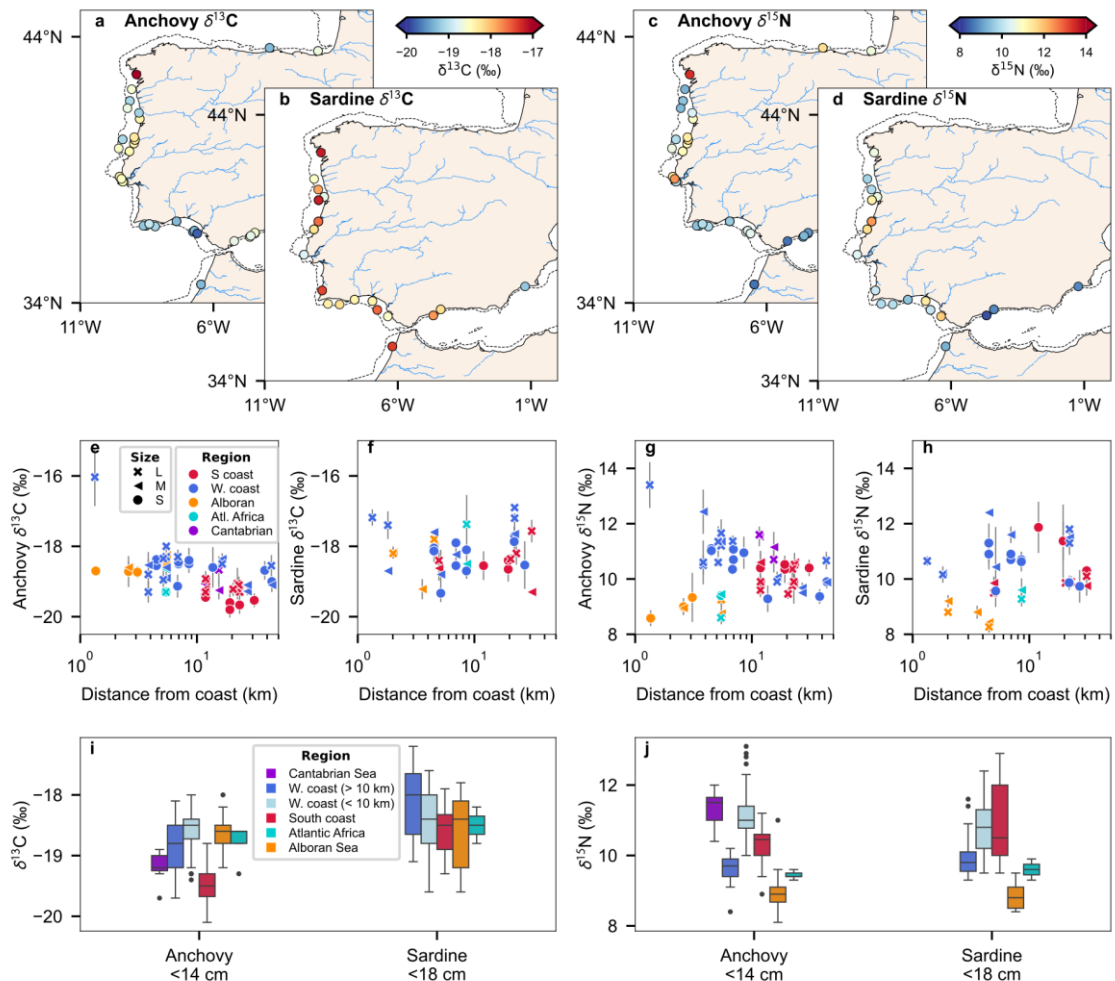
280
281 Natural logarithms of abundance indices ($\ln(N+k)$) per age were compared between the
282 contiguous areas by adjusting a linear regression model to the data, where N is number
283 of individuals at age and K is half the minimum but non-zero N observed for scaling. The
284 abundance-at-age was compared either for individuals of same age in a given year for
285 different areas (corresponding to matching dynamics of cohorts) or comparing the
286 abundance of individuals at age x and year y in a given area, with the abundance of
287 individuals of age $x+1$ in year $y+1$ in the contiguous area (testing for migration from one
288 area to the other during the time between surveys). Correlations were tested between the
289 Cantabrian Sea and the West coast and between the West coast and the South coast.

290
291 **Results**

292 *Muscle isotope distribution*

293 The $\delta^{13}\text{C}$ and $\delta^{15}\text{N}$ values of the muscles of anchovy (70–184 mm TL) and sardine (104–
294 220 mm TL) showed significant variations among and within regions (Fig. 2a–j). The
295 $\delta^{13}\text{C}$ value ranged from $-20.1\text{\textperthousand}$ to $-15.6\text{\textperthousand}$ in anchovy and from $-19.6\text{\textperthousand}$ to $-16.2\text{\textperthousand}$ in
296 sardine, with the general tendency of higher values in sardine (Fig. 2a, c). The $\delta^{15}\text{N}$ values
297 ranged from $+8.1\text{\textperthousand}$ to $+14.1\text{\textperthousand}$ and from $+8.1\text{\textperthousand}$ to $+12.9\text{\textperthousand}$ for anchovy and sardine,
298 respectively (Fig. 2c, d). Exceptionally high $\delta^{15}\text{N}$ anchovy were found for large
299 individuals (151–173 mm) caught during October 2022 in the Ría de Arousa estuary
300 ($+13.4 \pm 0.8\text{\textperthousand}$, Fig. 2a, c), and from medium individuals (124–134 mm) caught close to
301 the Tagus River estuary during March 2022, both in the West coast (Fig. 2c). As such,
302 only in the West coast, significant correlations were detected between anchovy $\delta^{13}\text{C}$ and
303 $\delta^{15}\text{N}$ and logarithm of distance from the coast ($\delta^{13}\text{C}$: Pearson's $r = -0.50$, $p = 7.7*10^{-3}$;
304 $\delta^{15}\text{N}$: Pearson's $r = -0.50$, $p = 1.5*10^{-6}$, $n = 27$), revealing the marked inshore-offshore
305 gradients there. The geographical variation of $\delta^{13}\text{C}$ was less clear, except for low values
306 of anchovy caught off the South coast and Cantabrian Sea, which were not observed for
307

308 sardine (Fig. 2i). On the other hand, $\delta^{15}\text{N}$ values were significantly different between
309 regions for both species, with higher values (10–12‰) mainly observed in the Cantabrian
310 Sea, inshore (< 10 km) the West coast and in the South coast. Moderate values (9–10‰)
311 were found offshore (> 10 km) the West coast and Atlantic Africa, and the lowest (< 9‰)
312 in the Alboran Sea (Fig. 2j), likely reflecting different isotope baselines across regions.



313

Figure 2. Variations of muscle isotopes. Station-mean $\delta^{13}\text{C}$ (a, b) and $\delta^{15}\text{N}$ (c, d) of anchovy (a, c) and sardine white muscles (b, d). Relationships between distance from coast and station/size class-mean $\delta^{13}\text{C}$ (e, f) and $\delta^{15}\text{N}$ (g, h) of anchovy (e, g) and sardine (f, h). Regional difference of $\delta^{13}\text{C}$ (i) and $\delta^{15}\text{N}$ (j) of small to medium anchovy and sardine, shown as boxplots. The west coast data is split into close or far from the coast at 10 km (i, j), given the significant gradient there (g).

314

315

316 *Eye lens isotopes*

317 The dry weight of delaminated eye lens centres ranged between 0.10 and 0.53 mg, whose
 318 effect on isotope values were assessed by linear model (Supplementary Table 1;
 319 Supplementary Fig. 1). For anchovy, the estimated slope of the effect was 1.14‰/mg for
 320 $\delta^{13}\text{C}$ and 6.71‰/mg for $\delta^{15}\text{N}$, likely reflecting the change of trophic position with growth.
 321 For sardine, the effect on $\delta^{13}\text{C}$ was not significant, while the effect on $\delta^{15}\text{N}$ was 4.78‰/mg.

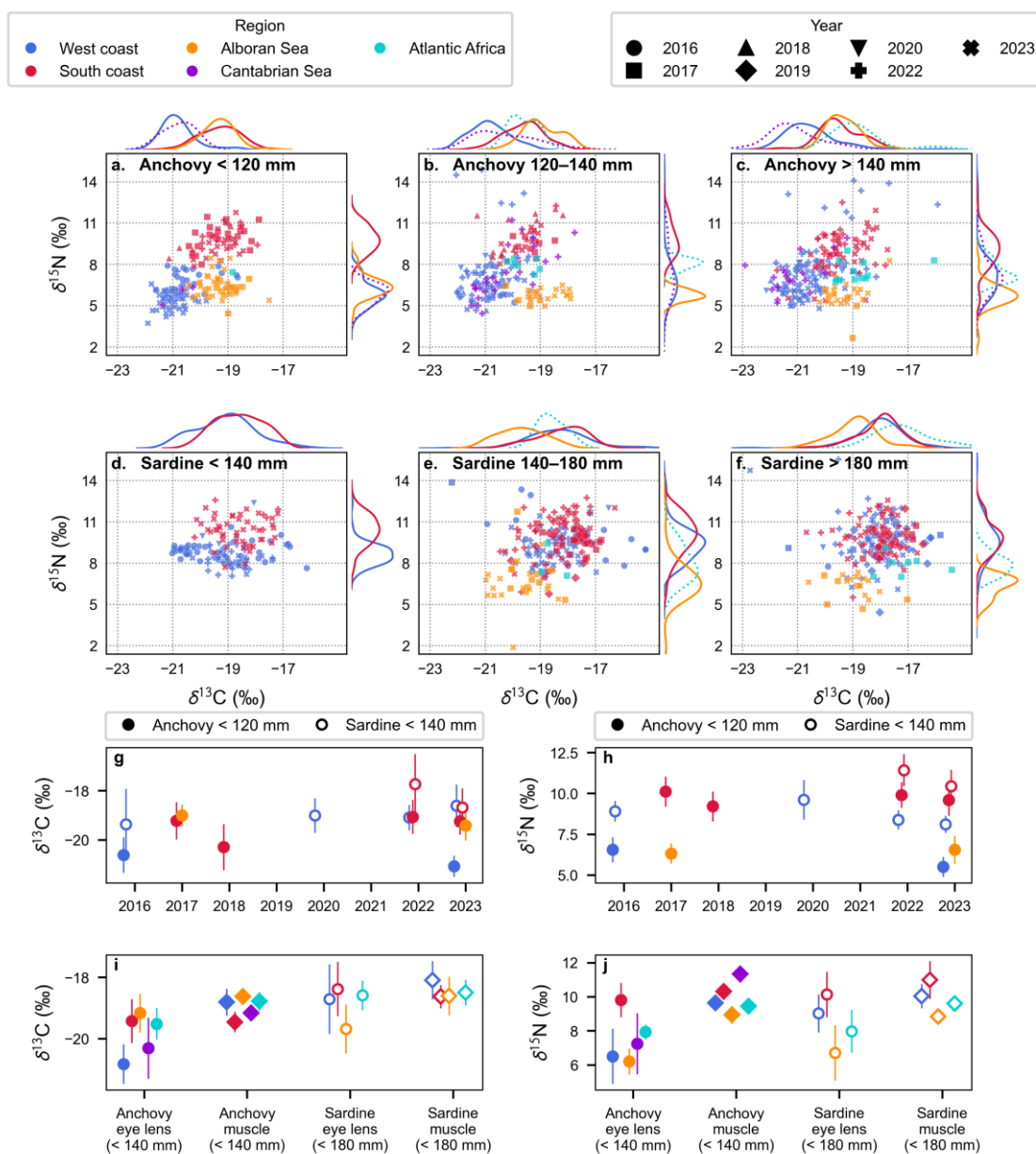
322 Hereafter, the eye lens $\delta^{13}\text{C}$ and $\delta^{15}\text{N}$ values corrected to those at 0.3 mg of sample weight
323 using the slopes were used in downstream analyses to account for this effect.

324

325 The $\delta^{13}\text{C}$ and $\delta^{15}\text{N}$ of eye lens centre values varied significantly by species, sampling area
326 and ontogeny (Fig. 3a–f). Anchovy showed distinct values between region, largely
327 consistent across size ranges (Fig. 3a–c): high $\delta^{15}\text{N}$ ($+9.6 \pm 1.3\text{\textperthousand}$ (1SD)) in the South
328 coast, lower $\delta^{15}\text{N}$ ($+6.8 \pm 1.8\text{\textperthousand}$) and $\delta^{13}\text{C}$ ($-20.7 \pm 0.8\text{\textperthousand}$) in the West coast, low $\delta^{15}\text{N}$
329 ($+5.9 \pm 0.8\text{\textperthousand}$) and higher $\delta^{13}\text{C}$ ($-19.2 \pm 0.6\text{\textperthousand}$) in the Alboran Sea, and moderate $\delta^{15}\text{N}$
330 ($+7.7 \pm 0.6\text{\textperthousand}$) and higher $\delta^{13}\text{C}$ ($-19.1 \pm 0.9\text{\textperthousand}$) in the Atlantic Africa. The Cantabrian Sea
331 showed values similar to those of the West coast, but also included higher ranges (Fig. 3b,
332 c). In sardine, $\delta^{13}\text{C}$ values showed less geographical variations and mostly fell in the range
333 between $-21\text{\textperthousand}$ and $-17\text{\textperthousand}$, though tended to be lower in the Alboran Sea (Fig. 3d–f). In
334 small sardine (< 140 mm), $\delta^{15}\text{N}$ values were higher in the South coast ($+10.1 \pm 1.3\text{\textperthousand}$)
335 and lower in the West coast ($+8.7 \pm 0.8\text{\textperthousand}$). This difference between the West and South
336 coasts decreased in medium and large sizes (Fig. 3d–f). In medium and large sardines,
337 $\delta^{15}\text{N}$ were lower in the Alboran Sea ($+6.5 \pm 1.6\text{\textperthousand}$) and moderate in the Atlantic Africa
338 ($+8.1 \pm 1.2\text{\textperthousand}$), and were distinct from those in the West and South coasts. Among
339 sampling years, mean eye lens isotope values of small anchovy and sardine in each region
340 varied by $< 1\text{\textperthousand}$ for $\delta^{13}\text{C}$ and $< 1.5\text{\textperthousand}$ $\delta^{15}\text{N}$, showing the robustness against inter-annual
341 variations. Compared to muscle isotopes, eye lens isotopes showed greater extent of
342 geographical variation (Fig. 4a, b). The difference of mean $\delta^{13}\text{C}$ in eye lens and muscle
343 for each region was less than 1\textperthousand in most cases, except for the West coast and Cantabrian
344 Sea anchovy that differed by $1\text{--}2\text{\textperthousand}$. The $\delta^{15}\text{N}$ were generally lower in eye lens centre by
345 $1\text{--}3\text{\textperthousand}$, although the ranks were mostly consistent between muscles and eye lens centres
346 if we use offshore (>10 km) mean for the West coast for the muscle (Fig. 4b). The
347 exception here was the Cantabrian Sea, where muscles showed highest $\delta^{15}\text{N}$ values but
348 lower in eye lenses.

349

350



351
352

Figure 3. Variations of eye lens centre isotopes. Eye lens centre $\delta^{13}\text{C}$ and $\delta^{15}\text{N}$ of anchovy (a, b, c) and sardine (d, e, f) of small (a, d), medium (b, e) and large size (c, f), where colours and symbols represent sampling regions and years, respectively. Inter-annual variations of eye lens $\delta^{13}\text{C}$ (g) and $\delta^{15}\text{N}$ (h) of small anchovy (filled) and sardine (open). Comparison of geographical differences in $\delta^{13}\text{C}$ (i) and $\delta^{15}\text{N}$ (j) between eye lens centre and muscle. The nearshore muscle data (< 10 km) in the West coast fishes are excluded given the strong inshore-offshore gradient there (i, j). The plots and error bars show mean and 1 SD, respectively (g-j).

353

354

355 The similarity of eye lens centre isotopes between regions, size classes and sampling year
356 were assessed as the overlaps of 2-D histograms (Fig. 4). For anchovy, higher overlaps
357 (> 0.5) were mostly observed within each sampling region and not between the regions
358 across size classes and years, except for the West coast and Cantabrian Sea that showed
359 high overlaps (Fig. 4a). These results are indicative of limited movements of anchovies
360 between the Atlantic Africa, Alboran Sea, South coast and West coast, and potential
361 mixing between the West coast and the Cantabrian Sea. Despite this general trend, there
362 were outliers in each region that suggest individuals of different origins (Fig. 4b). In the
363 West coast, high eye lens $\delta^{15}\text{N}$ outliers were found in hauls in the Ría de Arousa and close
364 to the Tagus River mouth (Fig. 4b, c), which mostly matched the exceptionally high
365 muscle $\delta^{15}\text{N}$ individuals (Fig. 4d). This suggests the individuals' strong preference for
366 coastal environment potentially throughout life stages. At around the western edge of
367 South coast (stations "14", "15" and "17", Fig. 4c), six large anchovies showed similar
368 isotope values with the Alboran Sea or West coast fishes (Fig. 4b), which are likely
369 migrants from the adjacent regions. Similarly, the three small individuals found in the
370 westmost station ("67") in the Alboran Sea with higher $\delta^{15}\text{N}$ may have originated from
371 the South coast.

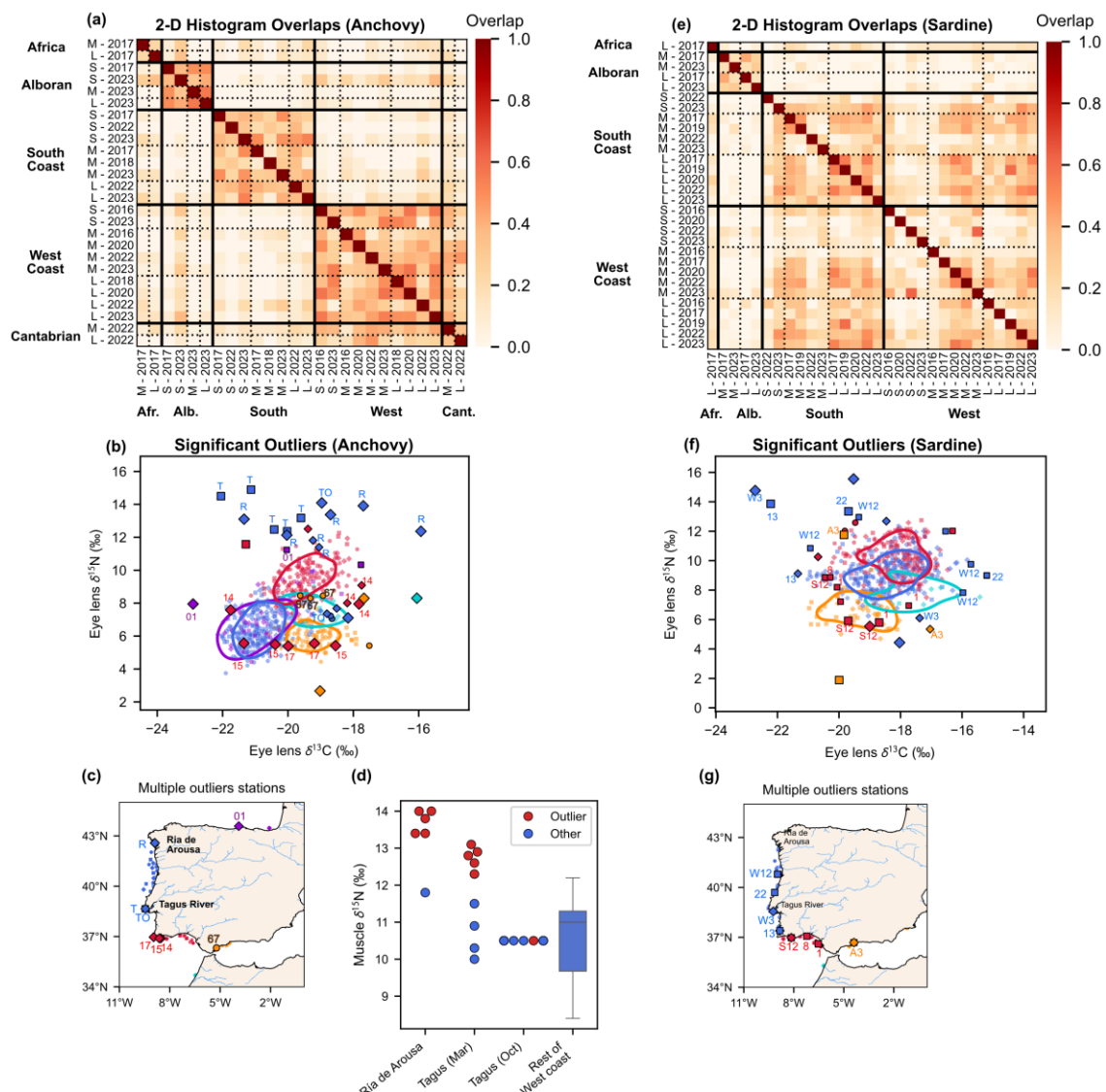
372

373

374 For sardine, higher histogram overlaps were shown within the Alboran Sea stations, but
375 also between medium to large individuals in the West and South coasts (Fig. 4e). These
376 are indicative of general separation between the Alboran Sea and the South coast at the
377 Strait of Gibraltar, and the mixing between the West and South coasts with age. The
378 highest overlap between the 2022 small and 2023 medium sardines stood up as an
379 exception, showing the strength of West coast recruits in 2022. Many of the outliers in
380 the West coast were collected in March 2016 ("W12", "22") in the low biomass period.
381 Outliers found in the South coast in 2022 ("S12") and 2019 ("1") with low $\delta^{15}\text{N}$ likely
382 originated from the Alboran Sea, showing the possibility of minor migration across the
383 Strait.

384

385



386

Figure 4. General trends and outliers of eye lens isotopes. Histogram overlaps between different sampling year/size class (Small, Medium, Large)/region groups for anchovy (a) and sardine (e). The outliers out of 95% (larger plots) and 99% (largest plots) confident ellipse based on Mahalanobis distance for each region, with small plots showing non-outliers and lines showing main data distributions based on kernel density estimation (50% probability mass area) for anchovy (b) and sardine (f). The annotations in (b, f) are station IDs from which multiple outliers were detected (c, g). The muscle $\delta^{15}\text{N}$ of West coast anchovy, with the detected high eye lens $\delta^{15}\text{N}$ outliers shown in red, others in blue plots or a boxplot.

387

388

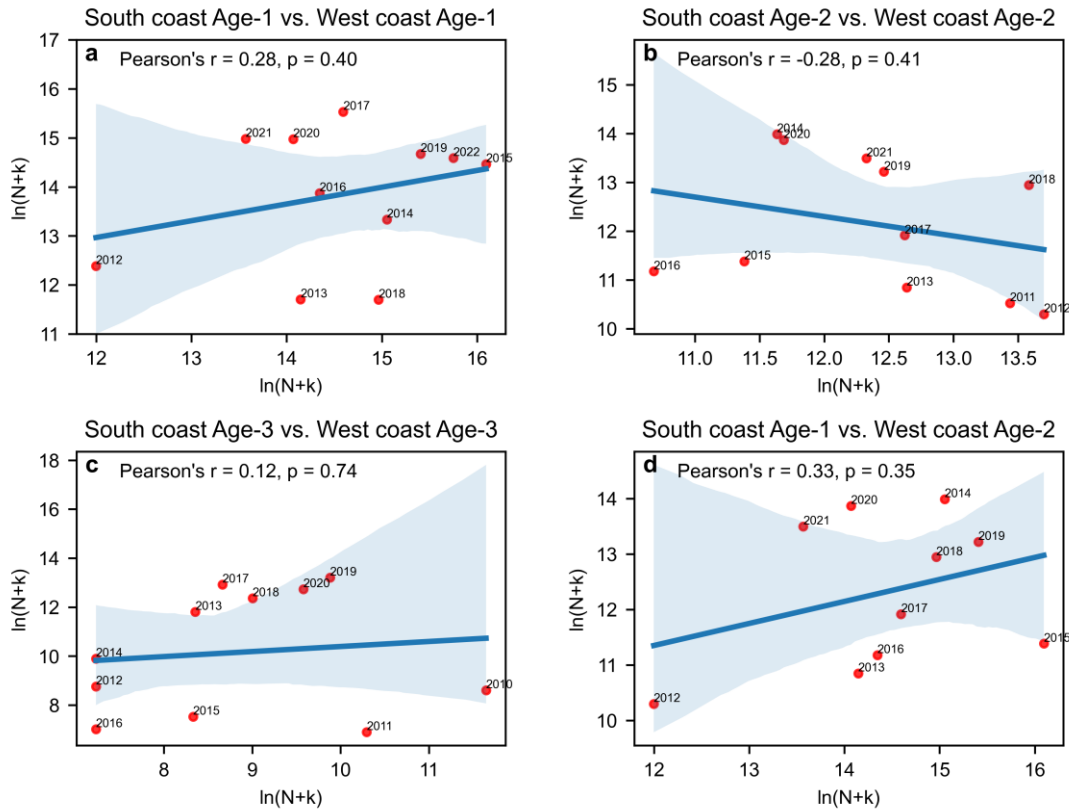
389

390

391 *Cohort tracking of anchovy*

392 Potential connectivity of anchovy populations from the North, West and South Iberia was
393 investigated by cohort tracking, comparing the abundance-at-age of fish from synoptical
394 spring acoustic surveys. The correlation of the abundance of fish from the West and South
395 Iberia was not significant for fish of the same age (p-values > 0.35, Fig. 5a, b, c).
396 Moreover, no significant correlation was found between age 1 individuals from the South
397 and age 2 individuals from the West in the following year (Fig. 5d), discarding the
398 hypothesis of a significant migration of recruits from the Gulf of Cadiz recruitment
399 hotspot to the West coast.

400



401

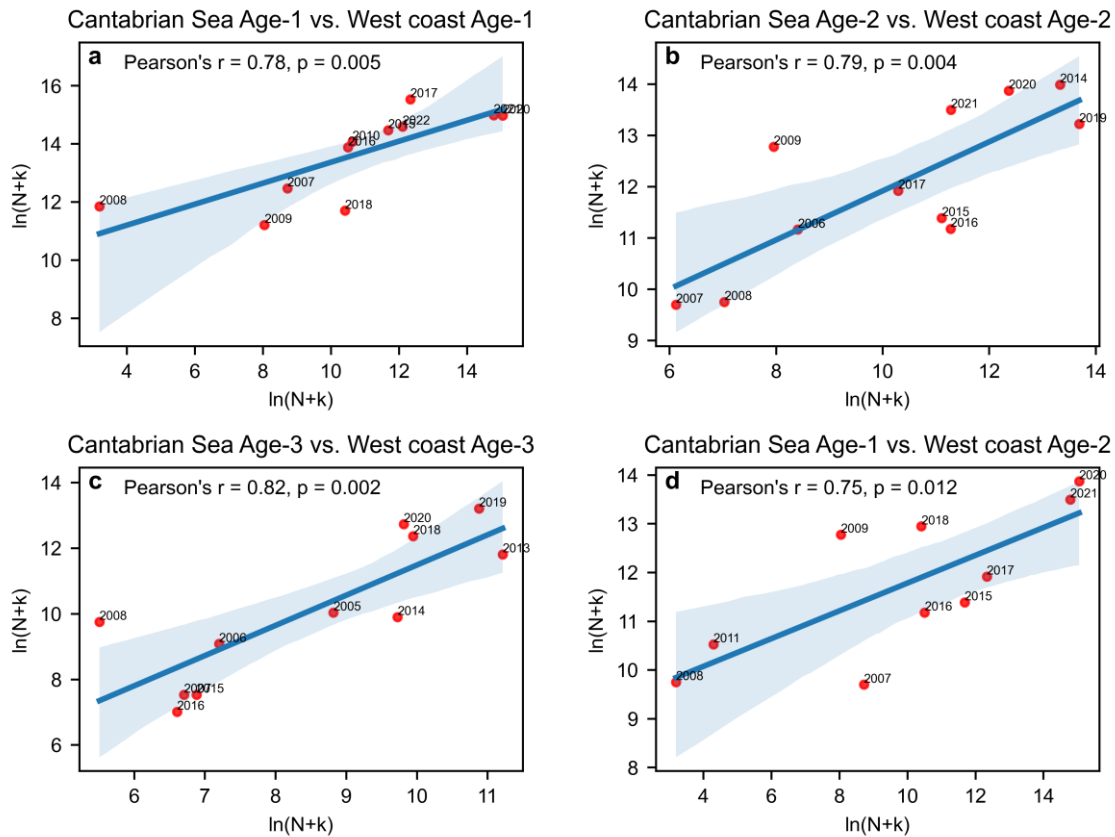
Figure 5. Cohort tracking of the West coast and South coast anchovies. Relationship between the abundance of Age 1, 2 and 3 individuals estimated in the PELAGO+PELACUS survey series in the West and the South Atlantic Iberian coast (a, b, c), and with Age 1 in the South and Age 2 in the West coast (d). Units for both axes are Log the number of individuals (N) + K, being K half the minimum non-zero N observed, method described in ICES, 2004; Payne et al., 2009). The labels represent year-classes.

402

403

404 The potential connectivity between the West coast and the North (Cantabrian Sea,
 405 corresponding to Division 8c which is part of the Bay of Biscay stock) was tested using
 406 the same approach. A significant correlation was found between the abundance of fish of
 407 the same age between both areas, for the three ages groups tested (p-values < 0.012, Fig.
 408 6a, b, c). Moreover, a significant correlation was found between age 1 individuals in the
 409 North with age 2 individuals found in the West Iberia in the following year, suggesting a
 410 potential southern migration during the juvenile stage (Fig.6d).

411



412

Figure 6. Cohort tracking of the West coast and Cantabrian Sea anchovies. Relationship between the abundance of Age 1, 2 and 3 individuals estimated in the PELAGO+PELACUS survey series and in the Cantabrian Sea (division 8c) (top panels and right bottom panel), and with Age 1 in the Cantabrian and Age 2 in the West Iberian coast (left bottom panel). Units for both axes are Log the number of individuals + K, being K half the minimum N observed, method described in ICES, 2004; Payne et al., 2009). The labels represent year-classes.

413

414

415 Discussion

416 In this study, we analysed the migration patterns of European anchovy and sardine around
 417 the Iberian Peninsula, by introducing stable isotopes of eye lenses for the first time for
 418 the species. The eye lens centre isotopes, particularly $\delta^{15}\text{N}$, were significantly different
 419 between recruitment areas around the Iberian Peninsula, thereby showing its utility as a
 420 marker of individual nursery origin in a shelf ecosystem of a scale of several-hundred
 421 kilometres. The analysis allowed to us to effectively visualise the overall mixing and
 422 separation patterns across regions that changed with ontogeny, and detected the outliers
 423 representing rare migrants or different ecotypes. With the support from cohort tracking

424 analysis, our results revealed the difference in migration ecology between the two small
425 pelagic species of similar niches, which have important implications for management.

426
427
428 The geographical variations of eye lens isotopes are mainly driven by difference in primary
429 producer isotopes. The eye lens centre record body isotope values during larval stage with several permill offset in $\delta^{15}\text{N}$ (Sakamoto et al., 2025), which sensitively reflects local prey isotopes in a short time period (Sakamoto et al., 2023a). This explains the lower $\delta^{15}\text{N}$, and similar but more exaggerated geographical isotopic differences in eye lenses than in muscles of juveniles and adults (Fig. 3). The important factors affecting phytoplankton isotopes are nutrient source and availability for $\delta^{15}\text{N}$ (Minagawa and Wada, 1986; Montoya and McCarthy, 1995), and temperature-dependent phytoplankton growth rates for $\delta^{13}\text{C}$ (Rau et al., 1989). The lower $\delta^{15}\text{N}$ in the Alboran Sea likely reflect the contribution of nitrogen originated from N_2 fixation that are active in the Mediterranean (Béthoux and Copin-Montégut, 1986). In contrast, the higher $\delta^{15}\text{N}$ in the West coast nearshore waters likely reflects inputs from anthropogenic origin nitrogen that has high $\delta^{15}\text{N}$ (Vinagre et al., 2011; Bode et al., 2025). On the other hand, the West coast and Atlantic Africa are both part of Canary Current upwelling system, where abundant nutrients supplied from deep waters. Preferential uptake of lighter nitrogen by phytoplankton from a rich pool likely led to the lower baseline $\delta^{15}\text{N}$ there, which may have worked otherwise in the nutrient-limited South coast. For $\delta^{13}\text{C}$, lower values in anchovy eye lens in the Cantabrian Sea and the West coast likely reflect lower nursery temperatures than in southern areas. Trends in $\delta^{13}\text{C}$ were inconsistent across species and tissues, suggesting that the spatial differences in baselines can be outweighed by species or life-stage dependent factors such as spawning seasonality or local-scale habitat selection particularly near river mouth. The results for the Cantabrian Sea anchovy were unexpected, having high $\delta^{15}\text{N}$ and moderate $\delta^{13}\text{C}$ in muscle but both lower in eye lens centres (Fig. 3j). This is attributable to the unique movement pattern of anchovy there, where some individuals spend their early life stage off the shelf before migrating back closer to the coast (Irigoién et al., 2008), where zooplankton $\delta^{15}\text{N}$ and $\delta^{13}\text{C}$ are likely lower.

455
456 A self-recruiting anchovy population likely exists in the South Atlantic coast of Iberian
457 Peninsula. The separations of eye lens centre isotopes between the Atlantic Africa,
458 Alboran Sea, South coast and West coast–Cantabrian Sea regions, consistently evident
459 across different size classes and sampling years, suggest limited migrations across these

460 regions. The separation between the West and South coasts is also corroborated with the
461 lack of correlations of abundance at ages between the two areas (Fig. 5). While our
462 analyses cannot reject the mixing during larval stage via ocean transport (Casaucao et al.,
463 2021), the genomic differentiation between fish from the West and South coasts also
464 suggest the separation there (Pujolar et al., 2025). The Strait of Gibraltar, between the
465 South coast and the Alboran Sea, have not been identified as a significant barrier of gene
466 flow (Zarraonaindia et al., 2012; Alexandridis et al., 2025), although distinct otolith
467 morphometrics have been detected (Bacha et al., 2014), consistently with our inference
468 from eye lens isotope. Importantly, the existence of some large-sized migrants in the
469 western part of the South coast, likely from the West coast or the Alboran Sea, suggest
470 that the separation is not complete. As large anchovies are often collected as a minor
471 portion of a mixture with other species such as sardine and chub mackerels in trawl
472 surveys in the area (0.03–12% in 2023 PELAGO survey, ICES, 2024b), they may have
473 been trapped in the schools of larger fishes (Bakun and Cury, 1999) and taken to the area.
474 However, given the lack of such migrants in the Gulf of Cadiz, the eastern part South
475 coast where the major spawning activities in the South coast occur, the impact of the
476 migrants on abundance are likely limited. This line of evidence supports the recent
477 decision to split the South coast from the West coast stocks (ICES, 2024a) and different
478 managing units.

479
480 The anchovy populations in the West coast likely have a more complex structure. Despite
481 the current management assumption of considering the West populations as a stock unit,
482 the existence of a self-recruiting population here is disputable, as shown in the recent
483 genomic analysis that have suggested connectivity between anchovies from the West
484 coast and Ireland (Pujolar et al., 2025). Larval dispersal simulations also suggest that the
485 rapid population increase in the West coast since 2015 may be a result of colonisation
486 from Bay of Biscay populations, driven by anomalously strong and persistent westward
487 currents that occurred in the Cantabrian Sea in 2014 and 2015 (Teles-Machado et al.,
488 2024). Eye lens $\delta^{13}\text{C}$ and $\delta^{15}\text{N}$ were overlapping between anchovies in the West coast and
489 the Cantabrian Sea even in small sizes, but there was a discrepancy between $\delta^{13}\text{C}$ of eye
490 lens centre and muscle in the West coast (Fig. 3i). This can be reasonably explained if
491 most of the West coast anchovy spent their early life stage in the Cantabrian Sea and then
492 moved to the West coast. Moreover, the significant correlation of abundance at age
493 between the west and north Iberian coasts (Fig. 6) support the mixing. The western and
494 northern populations are currently managed as two independent stock units, but it is
495 advised to review stock limits, which is critical as underlying basis of stock assessment

496 and fisheries management. The West coast is characterised by frequent and strong coastal
497 upwelling events during spring and summer months, which provides a cooler and
498 productive environment for the mid-latitude area, with potential to host a population
499 adapted to higher latitudes.

500
501 Furthermore, the high $\delta^{15}\text{N}$ individuals in the Ría de Arousa and Tagus River estuaries
502 may be coastal ecotypes such as the ones identified in the Bay of Biscay, Mediterranean
503 Sea and North Sea (Huret et al., 2020; Le Moan et al., 2016) and have not been recognised
504 yet in the West coast. The impact of the estuarine ecotypes on stock assessment is likely
505 limited, as they were only found in low proportions. As the scattered estuarine ecotype
506 populations are known to be genetically differentiated while having a shared ancestry,
507 however, they deserve attention for conservation of genetic diversity. These are the
508 remaining issues for West coast anchovy managements that need to be solved by future
509 investigations, which should include whole-genome sequencies (e.g., Pujolar et al., 2025)
510 with spatially dense sampling, and inferences about individual movement histories based
511 on otolith oxygen isotopes (Sakamoto et al., 2024).

512
513 Sardine likely have broader migration ranges than anchovy. The previous cohort tracking
514 analysis across the Bay of Biscay shelf and the Iberian coasts predicted significant
515 migrations of sardines of age 1 to 3 among adjacent areas (Silva et al., 2019). The
516 converged eye lens isotope distributions of larger sardines in the West and South coasts,
517 despite the difference in small sardines, suggest the gradual ontogenetic mixing with age,
518 thereby providing empirical support for the prediction. The stock biomass of Iberian
519 sardine is under recovery from the historical low-levels during the 2010s. The suggested
520 mixing of the medium and large sardines in 2020s indicates that the recruitment hotspots
521 off the West and South coasts that respond differently to environmental variabilities
522 (Ferreira et al., 2023) both contributed significantly to the recovery, showing the
523 importance of the both for population fluctuations. Migrations though the Strait of
524 Gibraltar may occur occasionally from the East to the West against the Atlantic Jet, as a
525 minor number of outlier individuals with low eye lens $\delta^{15}\text{N}$ similar to the those in Alboran
526 Sea can be found in the South coast. The migrants may mediate gene flows suggested by
527 genomic studies (da Fonseca et al., 2024; Sabatino et al., 2025), although their low
528 proportions suggest limited impact on abundance. For practical management and stock
529 assessment, therefore, we present results support the assumption of a single
530 metapopulation extending from the north, west and south Iberian coasts, and splitting the
531 Alboran Sea and Africa.

532

533 The distinct migration patterns of sardines and anchovies off the Iberian Peninsula are
534 likely influenced by a combination of ecological and physiological factors. Anchovy
535 experience peak spawning in the spring and summer months, when upwelling events
536 enhance productivity, especially along the West coast where they are frequent and intense.
537 On the South coast, upwelling events occur less often and with lower intensity. Anchovy
538 larvae require higher energy intake to meet their physiological demands by developing in
539 warmer temperatures. Therefore spawning in the proximity of river runoff might be
540 essential, and this requirement to find such spawning locations for adults can limit their
541 migration far away from nursery areas. In contrast, sardines typically spawn between
542 October and March in colder waters, a period when downwelling conditions dominate off
543 western Iberia. The reduced metabolic costs of larvae in lower temperatures may relax
544 selections for spawning location of spawners, which may allow the adults to migrate more
545 freely to maximise energy acquisition. This is consistent with the view that sardine in the
546 European Atlantic do not show natal homing for spawning (Silva et al., 2019). Leaving
547 the nursery area and reproducing in other area has also been observed in *Sardinops* species
548 off South Africa coast and in the western North Pacific (Teske et al., 2021; Sakamoto et
549 al., 2025), which could be a general feature of sardines.

550

551 The different migration ecology of anchovy and sardine indicates that significant changes
552 in their abundance, which have been observed elsewhere (Chavez et al., 2003), can have
553 ecosystem-level impacts. Anchovy and sardine are both predominant zooplankton feeders
554 that prey on secondary productions and transfer the energy to higher trophic levels. Their
555 migrations from a nursery to different regions is therefore an energy export, suggesting
556 that the primary production in migration source areas can enrich higher level production
557 in the sink neighbouring areas (Hutchings et al., 2010). The excretion and death of fish in
558 the sink can also enhance nutrient recycling (Bauer and Hoye, 2014). The greater ability
559 of sardine to migrate suggests that the lateral energy transfer process would be
560 pronounced under sardine dominant condition and less in anchovy flourishing
561 environment. This leads to the hypothesis that the distribution and abundances of high
562 trophic level predators can be geographically more homogenised under sardine-
563 dominance but patchier and more concentrated under anchovy-dominance. Future
564 quantifications of the biomass of migrants, which could be predicted by cohort tracking
565 (Silva et al., 2019) and calibrated by eye lens isotopes analyses as in this study, may allow
566 assessments of the significance of the processes when combined with ecosystem models
567 (Veiga-Malta et al., 2019). This quantification should also be of great help to develop

568 spatial explicit management, which is crucial in the Iberian shelf system with significant
569 environmental heterogeneity.

570
571 Overall, we demonstrated that the stable isotopes in eye lenses are useful to understand
572 movement dynamics of marine fish. Given the similar isotopic trends between species,
573 the method would also be applicable for other species around Iberian Peninsula, and
574 beyond. Using only two isotope values for broader geographical range, however,
575 increases the risk of confusion of different nursery areas accidentally showing similar
576 values through different dynamics. The combination with other natural tags is therefore
577 the key for geographical expansions. Nevertheless, eye lens isotopes would remain an
578 important option due to the feasibility to generate large dataset, which allows to resolve
579 spatiotemporally varying mixing processes (Sakamoto et al., 2025). Such analysis allows
580 to remove spatial components from the temporal variation of population dynamics, which
581 would be of significant help to understand and predict marine fish population fluctuations.
582 in shorter time scales than molecular techniques, which is paramount to be able to cope
583 with rapid changes of fish distribution due to climate change and for spatially explicit
584 management.

585
586 **Acknowledgement**

587 This work was funded by project SARDINHA2030 (MAR-111.4.1-FEAMPA-10005),
588 from the Programa Operacional MAR 2030 (Portugal), and JSPS KAKENHI Grant
589 numbers 22H05028 and 23H02288 and the Hakubi Project, Kyoto University (Japan).
590 We thank the Portuguese Biological Sampling Program from the EU Data Collection
591 Framework (PNAB/DCF) funded by the European Maritime and Fisheries Fund through
592 the national operational program MAR2030. The authors are also in dept to colleagues
593 from the IEO-CSIC and AZTI for providing samples from Spanish waters. This work is
594 a contribution to the Working Group on Small Pelagic Fish started jointly by ICES
595 (WGSPF) and PICES (WG53).

596
597 **CRediT authorship contribution statement**

598 **Tatsuya Sakamoto:** Writing – review & editing, Writing – original draft, Visualization,
599 Validation, Methodology, Investigation, Funding acquisition, Formal analysis, Data
600 curation, Conceptualization. **Susana Garrido:** Writing – review & editing, Validation,
601 Methodology, Investigation, Funding acquisition, Formal analysis, Data curation.

602
603 **Data availability**

604 Data will be made available on request.

605

606 **References**

607 Alexandridis, D., Manousaki, T., Antoniou, A., Kristoffersen, J., Apostolidis, C.,
608 Cannas, R., Spedicato, M., Cariani, A., Bellido, J., Magoulas, A., Ramírez, F., Lloret-
609 Lloret, E., Albo-Puigserver, M., Coll, M., & Tsigenopoulos, C. (2025). Uncovering
610 the Genetic Structure of European Anchovy Populations in Central and Western
611 Mediterranean. *Ecology and Evolution* 15(11): e72441. doi.org:10.1002/ece3.72441

612 Allen, G. H., & Pavelsky, T. M. (2018). Global extent of rivers and streams. *Science*,
613 361(6402), 585–588. doi:10.1126/science.aat0636

614 Bacha, M., Jemaa, S., Hamitouche, A., Rabhi, K., & Amara, R. (2014). Population
615 structure of the European anchovy, *Engraulis encrasicolus*, in the SW Mediterranean
616 Sea and the Atlantic Ocean: evidence from otolith shape analysis. *ICES Journal of*
617 *Marine Science*, 71(9), 2429–2435. doi:10.1093/icesjms/fsu097

618 Bakun, A., & Cury, P. (1999). The “school trap”: a mechanism promoting large-
619 amplitude out-of-phase population oscillations of small pelagic fish species. *Ecology*
620 *Letters*, 2(5), 349–351. doi:10.1046/j.1461-0248.1999.00099.x

621 Bauer, S., & Hoye, B. J. (2014). Migratory animals couple biodiversity and ecosystem
622 functioning worldwide. *Science*, 344(6179), 1242552. doi:10.1126/science.1242552

623 Berger, A. M., Deroba, J. J., Bosley, K. M., Goethel, D. R., Langseth, B. J., Schueller,
624 A. M., & Hanselman, D. H. (2020). Incoherent dimensionality in fisheries
625 management: consequences of misaligned stock assessment and population
626 boundaries. *ICES Journal of Marine Science*, 78(1), 155–171.
627 doi:10.1093/icesjms/fsaa203

628 Béthoux, J. P., & Copin-Montégut, G. (1986). Biological fixation of atmospheric
629 nitrogen in the Mediterranean Sea. *Limnology and Oceanography*, 31(6), 1353–1358.
630 doi:10.4319/lo.1986.31.6.1353

631 Bode, A., Álvarez-Ossorio, M. T., Cunha, M. E., Garrido, S., Peleteiro, J. B., Porteiro,
632 C., Valdés, L., & Varela, M. (2007). Stable nitrogen isotope studies of the pelagic

633 food web on the Atlantic shelf of the Iberian Peninsula. *Progress in Oceanography*,
634 74(2–3), 115–131. doi:10.1016/j.pocean.2007.04.005

635 Bode, A., García-Seoane, R., Varela, Z., & Viana, I. G. (2025). Assessment of decadal
636 changes in coastal nitrogen sources in NW Spain with stable isotopes in macroalgae
637 and mussels. *PLOS ONE*, 20(7), e0327159. doi:10.1371/journal.pone.0327159

638 Caballero-Huertas, M., Frigola-Tepe, X., Coll, M., Muñoz, M., & Viñas, J. (2022a). The
639 current knowledge status of the genetic population structure of the European sardine
640 (*Sardina pilchardus*): uncertainties to be solved for an appropriate fishery
641 management. *Reviews in Fish Biology and Fisheries*, 32, 745–763.
642 doi:10.1007/s11160-022-09704-z

643 Caballero-Huertas, M., Vargas-Yáñez, M., Frigola-Tepe, X., Viñas, J., & Muñoz, M.
644 (2022b). Unravelling the drivers of variability in body condition and reproduction of
645 the European sardine along the Atlantic–Mediterranean transition. *Marine
646 Environmental Research*, 179, 105697. doi:10.1016/j.marenvres.2022.105697

647 Cadrin, S. X., Goethel, D. R., Berger, A., & Jardim, E. (2023). Best practices for
648 defining spatial boundaries and spatial structure in stock assessment. *Fisheries
649 Research*, 262, 106650. doi:10.1016/j.fishres.2023.106650

650 Cardona, L., Martínez-Iñigo, L., Mateo, R., & González-Solís, J. (2015). The role of
651 sardine as prey for pelagic predators in the western Mediterranean Sea assessed using
652 stable isotopes and fatty acids. *Marine Ecology Progress Series*, 531, 1–14.
653 doi:10.3354/meps11353

654 Casaucao, A., González-Ortegón, E., Jiménez, M. P., Teles-Machado, A., Plecha, S.,
655 Peliz, A. J., & Laiz, I. (2021). Assessment of the spawning habitat, spatial
656 distribution, and Lagrangian dispersion of the European anchovy (*Engraulis
657 encrasicolus*) early stages in the Gulf of Cádiz during an apparent anomalous episode
658 in 2016. *Science of the Total Environment*, 781, 146530.
659 doi:10.1016/j.scitotenv.2021.146530

660 Chávez, F. P., Ryan, J., Lluch-Cota, S. E., & Ñiquen, C. M. (2003). From anchovies to
661 sardines and back: multidecadal change in the Pacific Ocean. *Science*, 299(5604),
662 217–221. doi:10.1126/science.1075880

663 Chouvelon, T., Violamer, L., Dessier, A., Bustamante, P., Mornet, F., Pignon-Mussaud,
664 C., & Dupuy, C. (2015). Small pelagic fish feeding patterns in relation to food
665 resource variability: an isotopic investigation for *Sardina pilchardus* and *Engraulis*
666 *encrasicolus* from the Bay of Biscay (north-east Atlantic). *Marine Biology*, 162, 15–
667 37. doi:10.1007/s00227-014-2577-5

668 da Fonseca, R. R., Campos, P. F., Rey-Iglesia, A., Barroso, G. V., Bergeron, L. A.,
669 Nande, M., Tuya, F., et al. (2024). Population genomics reveals the underlying
670 structure of the small pelagic European sardine and suggests low connectivity within
671 Macaronesia. *Genes*, 15(2), 170. doi:10.3390/genes15020170

672 FAO (2025). Fishery and Aquaculture Statistics – Yearbook 2023. FAO Yearbook of
673 Fishery and Aquaculture Statistics. Rome. 240pp. doi:10.4060/cd6788en

674

675 Ferreira, A., Brotas, V., Palma, C., Borges, C., & Brito, A. C. (2021). Assessing
676 phytoplankton bloom phenology in upwelling. *Remote Sensing*, 13(4), 675.
677 <https://doi.org/10.3390/rs13040675>

678 Ferreira, A., Garrido, S., Costa, J. L., Teles-Machado, A., Brotas, V., & Brito, A. C.
679 (2023). What drives the recruitment of European sardine in Atlanto-Iberian waters
680 (SW Europe)? Insights from a 22-year analysis. *Science of the Total Environment*,
681 881, 163421. doi:10.1016/j.scitotenv.2023.163421

682 Ferreira, A., Brito, A. C., Costa, J. L., Brotas, V., Teles-Machado, A., & Garrido, S.
683 (2024). Anchovy on the rise: investigating environmental drivers of recruitment
684 strength in the northern Canary Current. *Marine Ecology Progress Series*, 741, 315–
685 330. doi:10.3354/meps14594

686 Frisk, M. G., Jordaan, A., & Miller, T. J. (2014). Moving beyond the current paradigm
687 in marine population connectivity: are adults the missing link? *Fish and Fisheries*,
688 15(2), 242–254. doi:10.1111/faf.12014

689 Garrido, S., Silva, A., Pastor, J., Domínguez, R., Silva, A. V., & Santos, A. M. P.
690 (2015). Trophic ecology of pelagic fish species off the Iberian coast: diet overlap,
691 cannibalism and intraguild predation. *Marine Ecology Progress Series*, 539, 271–
692 285. doi:10.3354/meps11506

693 Garrido S, Rodríguez-Espeleta, N., Díaz, N., Machado, A., Sakamoto, T., Ramos, F.,
694 Rincón, M., Moreno, A., Jiménez, M., Santos, M., Carrera, P., Rodriguez-Climent,
695 S., Feijó, D., Ibarbarriaga, L., Cidores, L., Boyra, G., Duhamel E. (2024). Population
696 structure of the European Anchovy (*Engraulis encrasicolus*) In ICES Division 9a.
697 Working document presented to the ICES Stock Identification Methods Working
698 Group (SIMWG) and ICES Benchmark workshop on anchovy species (WKBANSP).

699 Hidalgo, M., Hernández, P. & Vasconcellos, M., eds. (2024). Transboundary population
700 structure of sardine, European hake and blackspot seabream in the Alboran Sea and
701 adjacent waters – A multidisciplinary approach. Studies and Reviews No. 104
702 (General Fisheries Commission for the Mediterranean). Rome, FAO.
703 doi:10.4060/cd1122en

704 Huret, M., Lebigre, C., Iriondo, M., Montes, I., & Estonba, A. (2020). Genetic
705 population structure of anchovy (*Engraulis encrasicolus*) in North-western Europe
706 and variability in the seasonal distribution of the stocks. *Fisheries Research*, 229,
707 105619.

708 Hutchings, L., Morris, T., van der Lingen, C. D., Lamberth, S. J., Connell, A. D.,
709 Taljaard, S., & van Niekerk, L. (2010). Ecosystem considerations of the KwaZulu-
710 Natal sardine run. *African Journal of Marine Science*, 32(2), 413–421.
711 doi:10.2989/1814232X.2010.502644

712 ICES. (2004). Report of the Study Group on Assessment Methods Applicable to
713 Assessment of Norwegian Spring-Spawning Herring and Blue Whiting Stocks
714 (SGAMHBW). 19-22 February 2004, Lisbon, Portugal. ICES CM 2014/ACFM 145.
715 166 pp.

716 ICES. (2024a). Benchmark Workshop on anchovy stocks (WKBANSP). *ICES Scientific*
717 *Reports*, 6(96), 511 pp. doi.org:10.17895/ices.pub.27909783

718 ICES. (2024b). Working Group on Southern Horse Mackerel, Anchovy and Sardine
719 (WGHANSA). *ICES Scientific Reports*, 6(46), 738 pp.
720 doi.org:10.17895/ices.pub.26003356

721 Irigoien, X., Cotano, U., Boyra, G., Santos, M., Álvarez, P., Otheguy, P., Etxeberria, E.,
722 et al. (2008). From egg to juvenile in the Bay of Biscay: spatial patterns of anchovy

723 (723) (*Engraulis encrasicolus*) recruitment in a non-upwelling region. *Fisheries*
724 *Oceanography*, 17(6), 446–462. doi:10.1111/j.1365-2419.2008.00492.x

725 (725) Lafuente, J. G., & Ruiz, J. (2007). The Gulf of Cádiz pelagic ecosystem: a review.
726 *Progress in Oceanography*, 74(2-3), 228-251. doi:10.1016/j.pocean.2007.04.001

727 (727) Le Moan, A., Gagnaire, P.-A., & Bonhomme, F. (2016). Parallel genetic divergence
728 among coastal–marine ecotype pairs of European anchovy explained by differential
729 introgression after secondary contact. *Molecular Ecology*, 25(14), 3187–3202.
730 doi:10.1111/mec.13627

731 (731) Link, J. S., Huse, G., Gaichas, S., & Marshak, A. R. (2020). Changing how we approach
732 fisheries: a first attempt at an operational framework for ecosystem approaches to
733 fisheries management. *Fish and Fisheries*, 21(2), 393–434. doi:10.1111/faf.12438

734 (734) Martínez-Abraín, A., Santidrián Tomillo, P., Mouriño, J., Tenan, S., & Oro, D. (2019).
735 Delayed predator–prey collapses: the case of black-legged kittiwakes and Iberian
736 sardines. *Marine Ecology Progress Series*, 631, 201–207. doi:10.3354/meps13164

737 (737) Minagawa, M., & Wada, E. (1986). Nitrogen isotope ratios of red tide organisms in the
738 East China Sea: a characterization of biological nitrogen fixation. *Marine Chemistry*,
739 19(3), 245–259. doi:10.1016/0304-4203(86)90026-5

740 (740) Montoya, J. P., & McCarthy, J. J. (1995). Isotopic fractionation during nitrate uptake by
741 phytoplankton grown in continuous culture. *Journal of Plankton Research*, 17(3),
742 439–464. doi:10.1093/plankt/17.3.439

743 (743) Neves, J., Veríssimo, A., Múrias Santos, A., & Garrido, S. (2023). Comparing otolith
744 shape descriptors for population structure inferences in a small pelagic fish, the
745 European sardine *Sardina pilchardus* (Walbaum, 1792). *Journal of Fish Biology*,
746 102(5), 1219–1236. doi:10.1111/jfb.15369

747 (747) Payne, M. R., Clausen, L. W., Mosegaard, H. (2009). Finding the signal in the noise:
748 objective data-selection criteria improve the assessment of western Baltic spring-
749 spawning herring. *ICES Journal of Marine Science*, 66(8), 1673–1680. doi:
750 10.1093/icesjms/fsp185

751 Petitgas, P., Secor, D. H., McQuinn, I., Huse, G., & Lo, N. (2010). Stock collapses and
752 their recovery: mechanisms that establish and maintain life-cycle closure in space and
753 time. *ICES Journal of Marine Science*, 67(9), 1841–1848.
754 doi:10.1093/icesjms/fsq082

755 Pujolar, J. M., Gardiner, C. E. C., von der Heyden, S., Robalo, J. I., Castilho, R., Cunha,
756 R., Henriques, R., & Nielsen, E. E. (2025). Resolving the population structure and
757 demographic history of the European anchovy in the Northeast Atlantic: tracking
758 historical and contemporary environmental changes. *Molecular Ecology*, 34(14),
759 e17829. doi:10.1111/mec.17829

760 Rau, G. H., Takahashi, T., & DeMarais, D. J. (1989). Latitudinal variations in plankton
761 $\delta^{13}\text{C}$: implications for CO_2 and productivity in past oceans. *Nature*, 341(6242), 516–
762 518. doi:10.1038/341516a0

763 Sabatino, S. J., Cabezas, M. P., Pereira, P., Garrido, S., Santos, A. M., Carneiro, M.,
764 Santos, P. T., et al. (2025). Inversions dominate evolution in the European sardine
765 (*Sardina pilchardus*) amid strong gene flow. *Molecular Ecology*, 34(17), e70027.
766 doi:10.1111/mec.70027

767 Sakamoto, T., Horii, S., Kodama, T., Takahashi, K., Tawa, A., Tanaka, Y., & Ohshima,
768 S. (2023a). Stable isotopes in eye lenses reveal migration and mixing patterns of
769 diamond squid in the western North Pacific and its marginal seas. *ICES Journal of*
770 *Marine Science*, 80(7), 2313–2328. doi:10.1093/icesjms/fsad145

771 Sakamoto, T., Kodama, T., Horii, S., Takahashi, K., Tawa, A., Tanaka, Y., & Ohshima,
772 S. (2023b). Geographic, seasonal and ontogenetic variations of $\delta^{15}\text{N}$ and $\delta^{13}\text{C}$ of
773 Japanese sardine explained by baseline variations and diverse fish movements.
774 *Progress in Oceanography*, 219, 103163. doi:10.1016/j.pocean.2023.103163

775 Sakamoto, T., Takahashi, M., Shirai, K., Aono, T. & Ishimura, T. (2024). Fisheries
776 shocks provide an opportunity to reveal multiple recruitment sources of sardine in the
777 Sea of Japan. *Scientific Reports* 14, 21722. doi:10.1038/s41598-024-72925-8

778 Sakamoto, T., Takahashi, M., Shirai, K., Kitajima, S., Isihimura, T. (2025). Eye lens
779 isotope tag reveal migration as a driver of Japanese sardine synchrony. *EcoEvoRxiv*.
780 doi:10.32942/X2J077

781 Santos, M. B., Saavedra, C., & Pierce, G. J. (2014). Quantifying the predation on
782 sardine and hake by cetaceans in the Atlantic waters of the Iberian Peninsula. *Deep-*
783 *Sea Research Part II: Topical Studies in Oceanography*, 106, 232–244.
784 doi:10.1016/j.dsr2.2013.09.040

785 Silva, A., Carrera, P., Massé, J., Uriarte, A., Santos, M. B., Oliveira, P. B., Soares, E., et
786 al. (2008). Geographic variability of sardine growth across the northeastern Atlantic
787 and the Mediterranean Sea. *Fisheries Research*, 90(1–3), 56–69.
788 doi:10.1016/j.fishres.2007.09.011

789 Silva, A., Garrido, S., Ibaibarriaga, L., Pawlowski, L., Riveiro, I., Marques, V., Ramos,
790 F., et al. (2019). Adult-mediated connectivity and spatial population structure of
791 sardine in the Bay of Biscay and Iberian coast. *Deep-Sea Research Part II: Topical*
792 *Studies in Oceanography*, 159, 62–74. doi:10.1016/j.dsr2.2018.10.010

793 Taboada, F. G., Chust, G., Santos Mocoroa, M., Aldanondo, N., Fontán, A., Cotano, U.,
794 Álvarez, P., et al. (2024). Shrinking body size of European anchovy in the Bay of
795 Biscay. *Global Change Biology*, 30(6), e17047. doi:10.1111/gcb.17047

796 Teles-Machado, A., Plecha, S. M., Peliz, A., & Garrido, S. (2024). Anomalous ocean
797 currents and European anchovy dispersal in the Iberian ecosystem. *Marine Ecology*
798 *Progress Series*, 741, 289–300. doi:10.3354/meps14526

799 Teske, P. R., Emami-Khoyi, A., Golla, T. R., Sandoval-Castillo, J., Lamont, T.,
800 Chiazzari, B., McQuaid, C. D., Beheregaray, L. B., & van der Lingen, C. D. (2021).
801 The sardine run in southeastern Africa is a mass migration into an ecological
802 trap. *Science advances*, 7, eabf4514. doi:10.1126/sciadv.abf4514

803 Uriarte, A., Rico, I., Villamor, B., Duhamel, E., Dueñas, C., Aldanondo, N., & Cotano,
804 U. (2016). Validation of age determination using otoliths of the European anchovy
805 (*Engraulis encrasicolus* L.) in the Bay of Biscay. *Marine and Freshwater Research*,
806 67(7), 951–966. doi:10.1071/MF15092

807 Vecchio, J. L., & Peebles, E. B. (2022). Lifetime-scale ontogenetic movement and diets
808 of red grouper inferred using a combination of instantaneous and archival methods.
809 *Environmental Biology of Fishes*, 105(12), 1887–1906. doi:10.1007/s10641-022-
810 01210-2

811 Veiga-Malta, T., Szalaj, D., Angélico, M. M., Azevedo, M., Farias, I., Garrido, S.,
812 Lourenço, S., Marçalo, A., Marques, V., Moreno, A., Oliveira, P. B., Paiva, V. H.,
813 Prista, N., Silva, C., Sobrinho-Gonçalves, L., Vingada, J., & Silva, A. (2019). First
814 representation of the trophic structure and functioning of the Portuguese continental
815 shelf ecosystem: insights into the role of sardine. *Mar Ecol Prog Ser*, 617-618, 323–
816 340. doi:10.3354/meps12724

817 Véron, M., Duhamel, E., Bertignac, M., Pawlowski, L., & Huret, M. (2020). Major
818 changes in sardine growth and body condition in the Bay of Biscay between 2003 and
819 2016: temporal trends and drivers. *Progress in Oceanography*, 182, 102274.
820 doi:10.1016/j.pocean.2020.102274

821 Vinagre, C., Mágua, C., Cabral, H. N., & Costa, M. J. (2011). Spatial variation in river
822 runoff into a coastal area—An ecological approach. *Journal of Sea Research*, 65(3),
823 362–367. doi:10.1016/j.seares.2011.02.003

824 Wallace, A. A., Hollander, D. J., & Peebles, E. B. (2014). Stable isotopes in fish eye
825 lenses as potential recorders of trophic and geographic history. *PLOS ONE*, 9(10),
826 e108935. doi:10.1371/journal.pone.0108935

827 Yoshikawa, C., Ogawa, N. O., Ishikawa, N. F., Yoneda, M., Yukami, R., Ito, S., &
828 Ohkouchi, N. (2025). Nitrogen and carbon isotopic relationships in the diet and eye
829 lenses of chub mackerel revealed in a laboratory rearing experiment. *Progress in
830 Earth and Planetary Science*, 12, 57. doi:10.1186/s40645-025-00731-5

831 Zarraonaindia, I., Iriondo, M., Albaina, A., Pardo, M. A., Manzano, C., Grant, W. S.,
832 Irigoien, X., & Estonba, A. (2012). Multiple SNP markers reveal fine-scale
833 population and deep phylogeographic structure in European anchovy (*Engraulis
834 encrasicolus* L.). *PLOS ONE*, 7(7), e42201. doi:10.1371/journal.pone.0042201

835

836

837 **Supplementary Information for: Different migration patterns of European anchovy**
838 **and sardine around Iberian Peninsula revealed by eye lens isotopes**

839
840 **Authors**

841 Tatsuya Sakamoto^{1,2*} and Susana Garrido¹

842
843 **Affiliations**

844 1. Instituto Português do Mar e da Atmosfera, Lisbon, Portugal

845 2. The Hakubi Center for Advanced Research, Kyoto, Japan

846
847 *Corresponding author

848 Email: sakamoto.tatsuya.3p@kyoto-u.ac.jp

849 Present address: Yoshidanihonmatsucho, Kyoto Sakyo-ku, Kyoto, 606-8316 Japan

850
851 **Contents**

852 Supplementary Figure 1

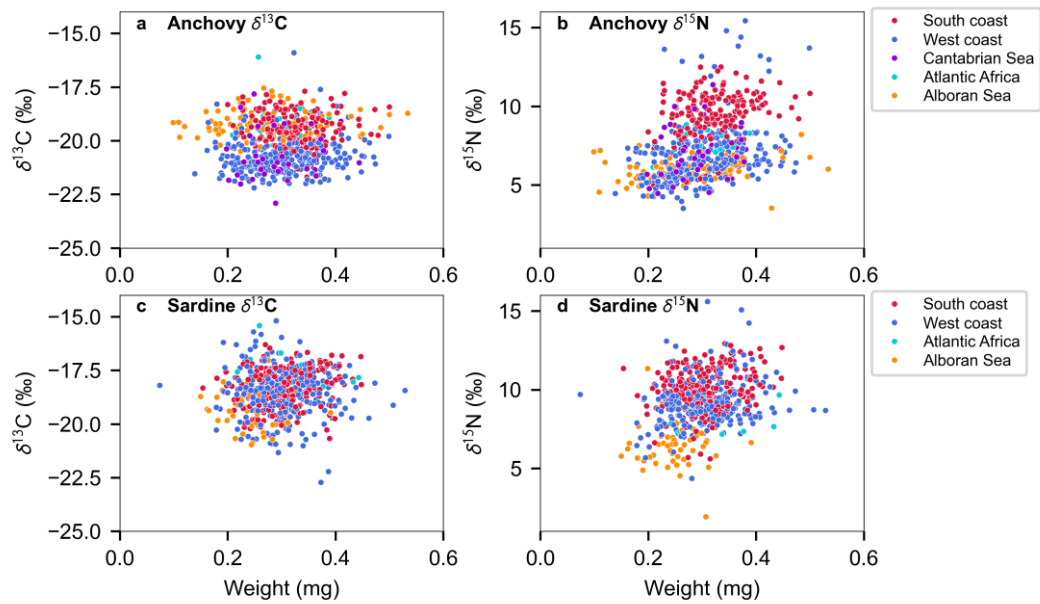
853 Supplementary Table 1

854

855

856

857



858

Supplementary Figure 1. The effect of sample weight on eye lens centre $\delta^{13}\text{C}$ (a, c) and $\delta^{15}\text{N}$ (b, d) in anchovy (a, b) and sardine (c, d). Colours indicate sampling region.

859

860

861

862

863 **Supplementary Table 1.**864 Summary results of linear model ($\delta^{13}C$ and $\delta^{15}N \sim$ Sample weight + Region).*Anchovy $\delta^{15}N \sim$ Sample weight + Region*

	Estimate	Std. Error	t-value	p-value	
(Intercept)	4.07	0.28	14.34	< 2E-16	***
Sample weight	6.71	0.88	7.59	1.2.E-13	***
Region:Atlantic Africa	1.58	0.36	4.40	1.3.E-05	***
Region:Cantabrian Sea	1.14	0.26	4.45	1.0.E-05	***
Region:South coast	3.36	0.19	17.80	< 2E-16	***
Region:West coast	0.76	0.17	4.39	1.3.E-05	***

Residual standard error: 1.46 on 621 degrees of freedom

Multiple R-squared: 0.483, Adjusted R-squared: 0.4788

F-statistic: 116 on 5 and 621 DF, p-value: < 2.2e-16

865

Anchovy $\delta^{13}C \sim$ Sample weight + Region

	Estimate	Std. Error	t-value	p-value	
(Intercept)	-19.55	0.15	-129.50	< 2e-16	***
Sample weight	1.14	0.47	2.43	0.016	*
Region:Atlantic Africa	0.12	0.19	0.61	0.54	
Region:Cantabrian Sea	-1.44	0.14	-10.51	< 2e-16	***
Region:South coast	-0.23	0.10	-2.29	0.022	*
Region:West coast	-1.50	0.09	-16.28	< 2e-16	***

Residual standard error: 0.7764 on 621 degrees of freedom

Multiple R-squared: 0.4403, Adjusted R-squared: 0.4358

866 F-statistic: 97.69 on 5 and 621 DF, p-value: < 2.2e-16

867

868 **Supplementary Table 1 (continued).***Sardine $\delta^{15}\text{N} \sim \text{Sample weight} + \text{Region}$*

	Estimate	Std. Error	t-value	p-value	
(Intercept)	5.30	0.31	17.16 < 2e-16		***
Sample weight	4.16	0.97	4.28	2.23E-05	***
Region: Atlantic Africa	1.33	0.47	2.89	0.0040	**
Region: South coast	3.50	0.22	16.09 < 2e-16		***
Region: West coast	2.70	0.21	12.66 < 2e-16		***

Residual standard error: 1.337 on 589 degrees of freedom

Multiple R-squared: 0.3551, Adjusted R-squared: 0.3508

F-statistic: 81.1 on 4 and 589 DF, p-value: < 2.2e-16

Sardine $\delta^{13}\text{C} \sim \text{Sample weight} + \text{Region}$

	Estimate	Std. Error	t-value	p-value	
(Intercept)	-19.43	0.24	-81.99 < 2e-16		***
Sample weight	0.18	0.75	0.25	0.81	
Region: Atlantic Africa	1.79	0.37	5.06	5.66E-07	***
Region: South coast	1.12	0.17	6.74	3.88E-11	***
Region: West coast	0.90	0.17	5.49	6.16E-08	***

Residual standard error: 1.061 on 589 degrees of freedom

Multiple R-squared: 0.07797, Adjusted R-squared: 0.07171

869 F-statistic: 12.45 on 4 and 589 DF, p-value: 9.932e-10

870